Siberian Branch of Russian Academy of Science
BUDKER INSTITUTE OF NUCLEAR PHYSICS

B.A. Knyazev, J.B. Greenly, D.A. Hammer

LASER-DRIVEN ATOMIC-PROBE-BEAM DIAGNOSTICS

Budker INP 98-100

NOVOSIBIRSK
1998

Laser-driven atomic-probe-beam diagnostics

B.A. Knyazev[*], *J.B. Greenly*[**] *D.A. Hammer*[**]

[*] Novosibirsk State University,
Budker Institute of Nuclear Physics, 630090 Novosibirsk, Russia

[**] Laboratory of Plasma Studies, Cornell University, Ithaca, NY 14583

Abstract

A new approach to measuring several key parameters in an intense ion diode which we call Laser-driven Atomic-probe-beam Diagnostic (LAD) is presented. It is based on laser excitation and/or ionization of a probe atomic beam, pre-injected in the region under study, of elemental composition different from the bulk ion beam. This method can be used to determine the electric field as a function of position and time, including the positions of anode and cathode plasma emission surfaces (in order to obtain the effective accelerating gap); the anode plasma areal density distribution; the rate of neutral gas ionization near the anode emission surface; and the regions in the diode which are "responsible" for increasing of the ion beam divergence. As possible probe beams, we suggest the use of lithium, sodium and, possibly, boron atoms, which can be excited with existing dye lasers. The diagnostic provides a means to measure diode quantities spectroscopically and by monitoring extracted probe ions simultaneously both with excellent spatial resolution. For example, with a lithium or sodium atom beam, a specific excited state is populated up to saturation (directly or stepwise) by the resonance radiation of one or two flashlamp-pumped dye lasers. Since the electric field strength is a function of time the laser spectrum must be sufficiently wide to excite fine-varying Stark components of a spectral line throughout the diode voltage pulse. Recording of spontaneous emission spectrum originating from this level can yield the electric field strength and the position of the anode plasma boundary. If, in addition, a precisely-focused laser-beam can be used to provide photoionization of alkali atoms that are excited to any one of the upper levels of the atom, the extracted alkali ions can be analyzed to give, for example, the electrostatic potential at the point of origin of the ion, or the ion divergence as a function of the point of its birth. The latter might allow us to study the influence of conditions in the accelerating gap on the origin of ion divergence. High time and space resolutions of the technique are provided by special geometry of atomic and laser beams cross-section, adequate field of view of the spectroscopic system, as well as "momentary" ionization of probe atoms at determined point by high-power ionizing laser. A variant of the experimental system for study of proton or lithium diodes is given. Estimations of spatial and temporal resolution for the system based on Thomson spectrometer using a MCP+scintillator detector are presented. The technique can be applied to study wide variety of devices including transmission lines and Z-pinches.

1 Introduction

High-voltage vacuum diodes of various configurations have been used widely for generation of high-power electron and ion beams. In these diodes, electric fields up to 10 MV/cm, magnetic fields of several Tesla, and electron and ion current densities of kA/cm^2 are produced. Dense, not fully ionized plasmas are generally produced at electrode surfaces, either intentionally, as ion or electron sources, or unavoidably, by explosive emission processes. The resulting dynamics of plasmas and accelerated particles in these diodes require noninvasive temporally (ns) and spatially (<mm) resolved diagnostics. The single most critical quantity for understanding of diode gap processes is probably the electric field, but magnetic field, charged particle orbits, and plasma motion including charge-exchange and ionization of neutrals are also of great importance.

In typical high power ion diode configurations it is highly beneficial to use spectroscopic methods for measurements. Y.Maron *et al.* [1] used a spectroscopic technique for the first direct measurements of the electric field distribution in a magnetically-insulated ion diode. They measured the Stark shift of spectral lines of doubly-ionized aluminum ions as they crossed a diode gap. This method, which can be called "passive Stark spectroscopy", can be applied only to ion diodes with specially selected ion composition. Moreover, its sensitivity is rather low due to the characteristics of electron transitions in heavy ions. In particular, the precision of the measurements in the above-cited work was 0.4 MV/cm.

Recently, similar experiments were carried out in the ion diode of the PBFA-II accelerator [2]. The Stark shift of the $3p$ level of lithium in electric field up to 10 MV/cm was determined in these measurements by "semi-active

Stark atomic spectroscopy", without resonance laser excitation of atoms, but with self-injection of probe "charge-exchange" atoms from the partially ionized anode plasma layer into the diode gap. The probe atoms were produced because of the absence of a dense plasma layer with zero electric field near the anode in these experiments. They provide the first detailed investigation of ion diode acceleration gap physics in high power pulses, and the first observations of Stark shifts in a 10 MV/cm field.

Though the diagnostic methods used for electric field measurements in ion diodes so far have been successful, they are not generally applicable. They cannot be applied, for example, to a proton-beam accelerator, nor could they be used in a lithium-beam accelerator with a dense, fully-ionized anode plasma. Furthermore, both of these techniques can provide measurements only along a line of sight, not at a "point". In Refs. [3, 4] a method for measurement of the electric field in diodes using probe atoms injected into the gap and excited by resonant laser radiation was described. In this technique, called Active Stark Atomic Spectroscopy (ASAS), the Stark splitting of a probe-atom spectral line enables a calculation of the electric field with high time and space resolution. Since the probe atom density is less than the density of the background gas, this technique would not disturb the diode. However, high sensitivity is provided by using resonant laser excitation to saturate the population of the upper level of transitions of interest. Because one can easily distinguish signal from noise by simply omitting the probe beam or tuning lasers away from resonance with transitions, a reliable measurement can be made.

In Refs. [5, 6] measurements of the electric field in the 6-cm diode gap of the U–1 electron-beam accelerator by the ASAS technique were briefly described. A lithium atomic probe beam was injected into the gap before the high-voltage was applied. Lithium levels with a principal quantum number $n = 4$ were excited through cascade transitions using two dye-lasers. The bandwidth of the second laser was sufficiently wide to excite the split components of interest. Spontaneous emission was recorded with 1 mm spatial resolution by a monochromator combined with a fiber-optic or electron-optic dissector. These experiments enabled a direct measurement of the electric field strength at the definite point as a function of time in the diode during a 6-μs, $\sim$1 MV voltage pulse. The electric field strength measured in these experiments was 200–300 kV/cm, and the cathode and anode emission surfaces were located as a function of time.

The ASAS diagnostic method can certainly be applied to ion-beam diodes. In practical realization of the technique one needs only to take into account the specific ion diode conditions, including a higher electric field strength and

the presence of electron and ion flows in the gap. Obviously, the higher the electric field, the lower the atomic levels to be used in an experiment. The other obvious requirement is to use as a probe atoms elements different from the ions accelerated. For example, in a lithium ion diode it is reasonable to use sodium atoms as a spectroscopic probe. The features of the ASAS diagnostic technique with sodium atoms are practically the same as previously described [4] diagnostics with lithium atoms, and we leave out of the scope of this paper description of the ASAS diagnostics with sodium atoms.

In this paper we concentrate on a further elaboration of the technique, which substantially enhances its capability. We suggest to convert this diagnostic from merely a spectroscopic to a spectroscopic-corpuscular one. We describe how locally produced probe ions can be used to measure of potential distribution across the diode as well as to study sources of ion beam divergence in the diode. This combination of ASAS and novel corpuscular diagnostics can be named **L**aser-driven **A**tomic-probe-beam **D**iagnostics (**LAD**).

2 Experimental configuration

Typical magnetically-insulated proton- or lithium- ion diodes consist of (see Fig. 1) an annular anode and a cathode assembly. The transverse radial insulating magnetic field in the accelerating gap is parallel to the anode surface. A high-voltage positive pulse is applied to the anode and ions extracted from the anode plasma are accelerated across the gap (along z-direction), through the cathode plasma sheath, to form an intense annular ion beam. We will describe application of the LAD diagnostics to study characteristics of such a diode.

The spectroscopic LAD diagnostic (ASAS) requires an atomic probe beam with two exciting laser beams. One can suggest many different configurations for atomic and laser beams in the diode depending on experimental goals, namely to measure time evolution of the electric field at a local point, or to take a snapshot of lines of equal electric field strength, or to detect the emission surfaces and so on (see [7]). One of possible configurations is shown in Fig. 1. Atomic and one or two laser beams cross each other along a certain "line" between anode and cathode layers. Spontaneous fluorescence of the higher atomic level from this line is collected with a lens (not shown) and imaged on the input slit of a spectrograph. Distribution of Stark splitting along the z-axis recorded by a frame camera at the output of the spectrometer gives the instantaneous electric field distribution across the diode.

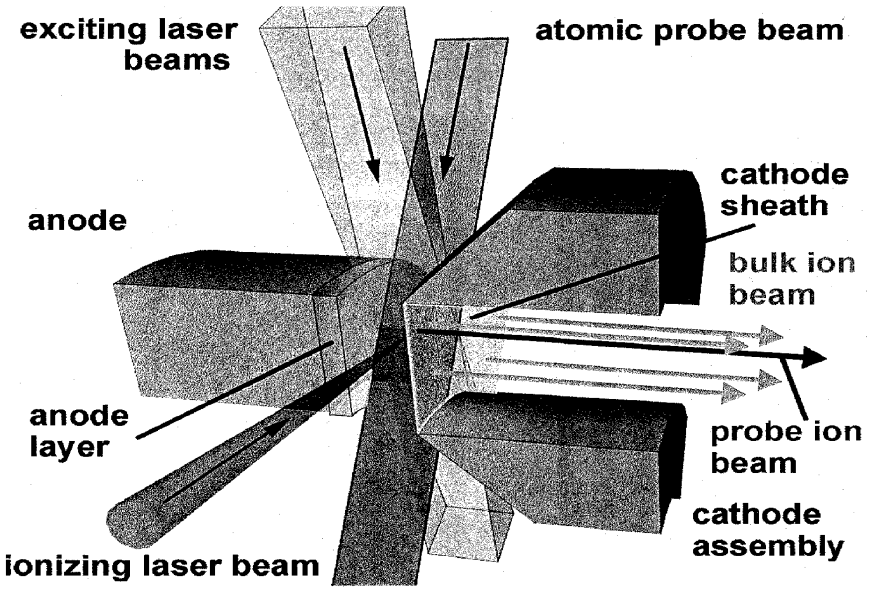

Figure 1: A sector of the anode-cathode gap of an ion beam diode is shown with the geometry of injection of atomic probe beam and laser beams for excitation (spectroscopic diagnostic) and ionization (probe ion diagnostic).

The angle between the atomic beam and two coinciding laser beams, as well the direction to the detector system, depends on features of the diode design, but it is better to provide crossing of the atomic and the laser beams rather close to a right angle. Then, with saturated population of the working level there is no problem with self-absorption of the resonance emission by the surrounding non-excited probe atoms (see [8]). Besides, when directions of excitation and obser vation are almost normal to the beam direction, one may ignore the Doppler-effect. A thin " ribbon-like" (of a rectangular cross-section with a small thickness in the direction of the laser beam) atomic probe beam would be the most satisfactory for such experiments. Depending on diode design the atomic beam can be injected to the gap normally to the anode or along the anode surface. A technique for formation of a ribbon-like atomic beam is described in [9].

3 Laser-driven Probe-Ion Diagnostics (LPID)

There are several possible measurement schemes for the particle diagnostics, but in all of them one can provide the local photoionization of excited probe atoms by a very intense laser beam at a specific location in the diode gap. The ions obtained in this way are accelerated in the applied electric field and can be detected after leaving the gap. By measurement of their energy, one can determine the potential at the ionization point. Measurement of the divergence of probe ions produced at different distances from the anode could locate the sources of the ion divergence. The key points in this diagnostic are (i) the selection of probe atoms, (ii) the choice of the ionizing laser, and (iii) the development of the methods of measurement of the probe ion characteristics.

Since the probe-ion time of flight out of the ion should be comparable with time of flight of bulk ions, possible probe atoms are limited to a few low-mass elements having resonance transitions which can be excited by available lasers to levels with a photoionization threshold less than the photon energy of the ionizing laser. Only three elements, lithium, sodium and, possibly, boron, whose partial Grotrian diagrams are shown in Fig. 2, satisfy these requirements. Time of flight τ_* of an ion which has been produced at a distance $\Delta z = d - z$ from the cathode is given by

$$\tau \simeq \sqrt{\frac{2Am_p(\Delta z)^2}{eU_*}} = 0.144\sqrt{\frac{A\,(\Delta z)^2[\mathrm{mm}]}{U_*[\mathrm{MV}]}}\ \ [\mathrm{ns}]\,, \qquad (1)$$

where A is an atomic number, U_* is a potential at this point at the moment,

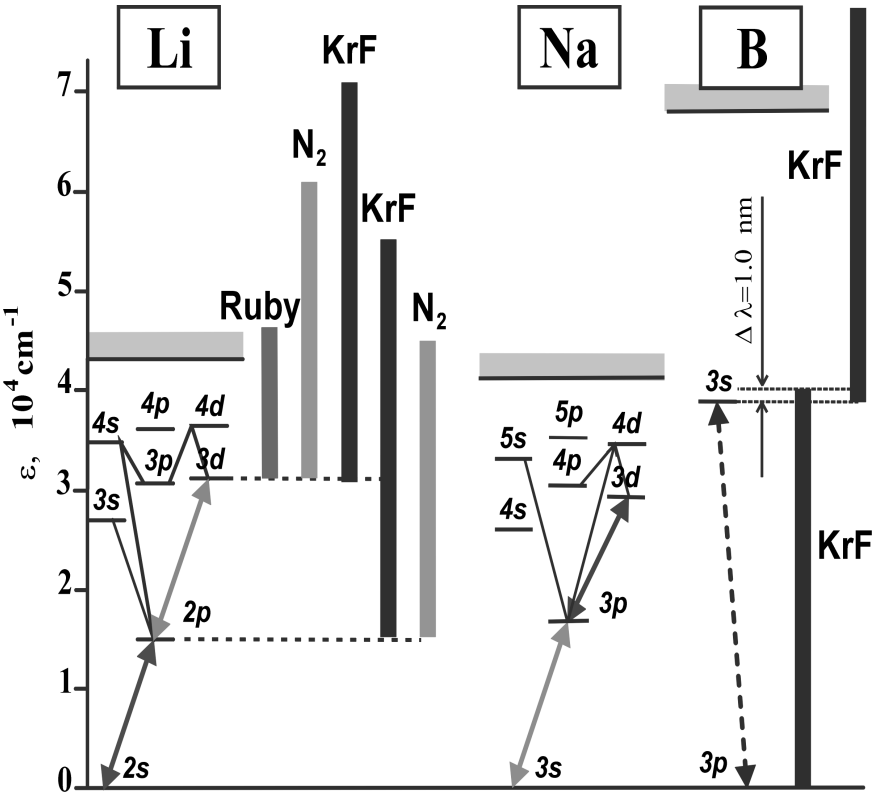

Figure 2: Atomic transitions of lithium and sodium which can be used for measurement of Stark splitting in high-voltage diodes. Bi-directional arrows indicate transitions excited to saturation by laser radiation. The bars give the photon energy of lasers that can be used for photoionization of excited atoms.

and d is anode–cathode separation. For U_*=1 MV and Δz=5 mm, time of flight for H^+ is 0.7 ns, Li^+ is 1.9 ns, B^+ is 2.3 ns, and Na^+ is 3.5 ns. Thus, lithium and boron can by used as probe ions in proton-beam diodes, and boron and sodium in the lithum-beam diodes.

4 Local production of probe ions by laser photoionization

Adequate sensitivity of LPID measurements can be obtained only when the working level(s) of the probe atoms is populated to saturation. Let us estimate intensities of exciting laser beams which provide saturation of the probe atom levels. Required laser spectral power density J_L^S can be determined from the kinetic equation for population of the higher level of a two-level system

$$\frac{dn_m}{dt} = n_n \int j_L(\omega)\,\sigma_{nm}(\omega)\,d\omega - n_m \int \left[j_L(\omega)\,\sigma_{mn}(\omega) + a_{mn}(\omega)\right]\,d\omega\ , \quad (2)$$

where

$$A_{mn} = \int a_{mn}(\omega)\,d\omega \quad (3)$$

is the first Einstein coefficient, and

$$\sigma_{nm}(\omega) = \frac{a_{mn}\,\lambda^2}{4} \quad (4)$$

is a cross-section of the induced radiation. Saturation of population corresponds to

$$j_L^S(\omega)\,\sigma_{mn}(\omega) = a_{mn}(\omega)\ , \quad (5)$$

whence a requirement for spectral power density of the exciting laser radiation $J_L^{ex}(\omega) \equiv j_L \cdot \hbar\omega$ follows

$$J_L^{ex}(\omega) \geq J_L^S(\omega) = \frac{4\hbar\omega}{\lambda^2} \quad \left[\frac{\mathrm{erg}}{\mathrm{cm}^2\ \cdot \mathrm{c} \cdot \mathrm{c}^{-1}}\right]\ . \quad (6)$$

Using a practical units and the relation $J_L(\lambda) = J_L(\omega) \cdot |d\omega/d\lambda|$, we obtain finally

$$J_L^{ex}(\lambda) \geq \frac{16\pi^2\hbar c^2}{\lambda^5} \quad \left[\frac{\mathrm{erg}}{\mathrm{cm}^2\ \cdot \mathrm{c} \cdot \mathrm{cm}}\right] \equiv \frac{1.42 \cdot 10^{14}}{\lambda^5\,[\mathrm{nm}]} \quad \left[\frac{\mathrm{kW}}{\mathrm{cm}^2 \cdot \mathrm{nm}}\right]\ . \quad (7)$$

Spectral power densities $J_L^S(\lambda)$ for the most interesting transitions of lithium, boron and sodium are given in the Table. These values are moderate for yellow and red spectral regions and can be easy obtained with conventional flashlamp-pumped dye lasers. Bandwidth of such lasers is about 1–3 nm [10] and their wavelength can be easy tuned to cover the wavelength of a resonance transition. Such tuning must be done with regard to Stark shift and splitting of the working levels in the electric field.

Table. Atomic transitions interesting for laser-driven diagnostics, photoionization cross-sections of the upper levels, and laser energy density necessary for photoionization of these levels.

Atom	Transition	λ, nm	J_L^S, kW/cm^2·nm	σ_{ph}, 10^{-18} cm^2 / $F_L \cdot \tau_i$, GW·ns/cm^2		
				KrF	N_2	Ru
Li	$2s$-$2p$	671	1.1	0.34/2.3	0.87/0.68	—
	$2p$-$3s$	813	0.4	0.085/9.4	0.21/2.8	—
	$2p$-$3d$	610	1.7	0.042/19	0.10/5.7	0.90/0.32
Na	$3s$-$3p$	590	2.0	0.20/3.9	0.51/1.2	—
	$3p$-$5s$	616	1.6	0.014/59	0.034/18	0.29/0.97
	$3p$-$4d$	819	0.39	0.037/217	0.091/6.5	0.80/0.36
B	$2p$-$3s$	249.8	150			

For production of probe ions an appropriate additional laser can be applied to photoionize a saturated excited level (or levels) of probe alkali atoms. Lasers with low-energy photons (ruby, neodymium), as shown in Fig. 2 for lithium, can ionize highly-excited atoms only. UV lasers (like KrF or N_2) can ionize all excited atoms. The photoionization cross-sections for atoms with one valence electron [11] can be determined from

$$\sigma_{ph} = 9 \cdot 10^{-18} \left(\frac{\varepsilon_n}{\hbar\omega_L}\right)^3 \frac{1}{(n - \Delta(n,l))^5} \ , \qquad (8)$$

where ω_L is laser radiation frequency, ε_n is photoionization threshold, and $\Delta(n,l)$ is quantum defect. Quantum defect for the alkali atoms does not depend on principle quantum number and for s, p, and d states of every n is equal to 0.40, 0.04, and 0.00 for Li and 1.37, 0.88, and 0.01 for Na, correspondingly. The cross-section increases dramatically for upper levels with high principal quantum numbers and rapidly decreases with increasing wavelength of the ionizing laser.

Levels of interest for ASAS technique in the electric field range from 0.1 to 10 MV/cm are $2p$, $3s$ and $3d$ for Li, and $3p$, $5s$ and $3d$ for Na. We will assume that the same excited levels are used for production of probe ions. Calculated photoionization cross-sections for these levels are given in the Table. For example, for KrF laser we have found $\sigma_{ph} = 3.4 \cdot 10^{-19}$ cm^2 for $2p$-level and $4.2 \cdot 10^{-20}$ cm^2 for $3d$-level of lithium. The upper transitions can be ionized with ruby and even neodymium lasers. For ruby laser the cross-section for $3d$ level is higher ($0.9 \cdot 10^{-18}$ cm^2) because the ratio $\varepsilon_n/\hbar\omega_L$ is close to unity.

Characteristic photoionization time is equal to $\tau_i = \nu_{ph}^{-1}$, where photoionization frequency ν_{ph} is

$$\nu_{ph} = \sigma_{ph}\ n_\varphi\ c\ . \tag{9}$$

From here

$$\tau_i = \frac{\hbar\omega}{n_\varphi\ \hbar\omega\ c\ \sigma_{ph}} = \frac{\hbar\omega}{F_L\ \sigma_{ph}}\ , \tag{10}$$

where F_L is power density of laser radiation, n_φ is photon density, and c is the speed of light. From this relation one can see that the product of ionization time and power density depends on $\hbar\omega$ and σ_{ph} only

$$\tau_i F_L = \frac{\hbar\omega}{\sigma_{ph}}\ . \tag{11}$$

As a result we have obtained a relation for estimation of critical laser power density for photoionization of probe atoms during a while τ_i

$$\tau_i\ [\text{ns}]\ \cdot\ F_L\ [\text{GW/cm}^2] = \frac{1.6 \cdot 10^{-19}\, \hbar\omega\ [\text{eV}]}{\sigma_{ph}\ [\text{cm}^2]}\ . \tag{12}$$

Values of this product are also presented in the Table.

To complete of this section let us mention alternative ways of photoionization of sodium and boron atoms in a high-voltage diode. The energy of KrF-laser photons lies within a band $40318 \div 40205$ cm^{-1} between $10p$ and $11p$ states of undisturbed sodium atom. That is only 1190 cm^{-1} less then ionization limit of a sodium atom. The level $10p$ is ionized by the electric field of $E_{cr} = 3.2 \cdot 10^8/(n - \Delta(n,l))^4 \approx 32$ kV/cm [12]. In the high field of the ion diode the Rydberg levels are widely split into many components. These components are densely distributed in energy space near the ionization limit. Therefore some of them at any time will coincide with the laser generation band. Thus excitation of these levels result in practically immediate field ionization. For the lithium KrF laser radiation lies close to $5p$ and $6p$ levels.

Because for $5p$ $E_{cr} \approx 1.1$ MV/cm, ionization of lithium atom by this way is questionable.

For boron the level system is quite different from the alkali atoms. Boron is not a hydrogen-like atom, and eq. (12) cannot be applied for calculation of photoionization. Nevertheless, one can expect that the cross-section of $3s$-state will be the same order of value as for the alkali atoms. A larger problem is excitation of boron atom to the $3s$-state. The only laser that can in principle excite this level is the KrF laser whose wavelength (λ= 248.1–248.8) is close to the $2p$–$3s$ resonance (249.7 nm) of boron. Though there is experimental evidence of excitation of atomic levels at a mismatch up to 2 nm (see, for example, [13]), this method must be verified experimentally. If it appears to be possible this system is very attractive for experiments, because one laser can be used simultaneously both for excitation and photoionization.

5 Application of LPID to measurement of divergence and local potential

One can suggest many experimental schemes based on LPID. We will discuss in this section the scheme shown in Fig. 3. For definiteness, we assume a 2-MV proton diode with electrode separation of about 5 mm. An atomic lithium probe beam of a width of 0.2 mm with a density of 10^{12} cm^{-3} is injected into the diode with small inclination in respect to direction of electric fields in the diode. Atoms of the beam are excited to an upper level, as described in section 2, by the resonant laser radiation (not shown in the figure). Radiation of an ionizing laser is focused to spot S =0.02 mm^2 at the atomic beam and produces in a small region (see the inset in the figure) probe ions by photoionization. This radiation does not affect the bulk ions and background atoms.

To achieve the highest sensitivity of probe ion detection as well excellent time resolution, the laser beam intensity has to provide complete ionization of probe atoms during a short time τ_i. In practice, τ_i should be not more then 1 ns, whereas characteristic laser pulse length τ_L is, usually, about 20 ns. Thus, requirement for energy of the ionizing laser is

$$\mathcal{E}_L\,[\mathrm{J}] = \frac{1.6\cdot 10^{-19}\,\hbar\omega\,[\mathrm{eV}]}{\sigma_{ph}\,[\mathrm{cm}^2]}\cdot\frac{\tau_L S}{\tau_i}\ . \tag{13}$$

For example, for the ruby laser, in accordance with Table 1, for lithium $3d$ state the necessary energy is 1 mJ only. Characteristic oscillograms of diode

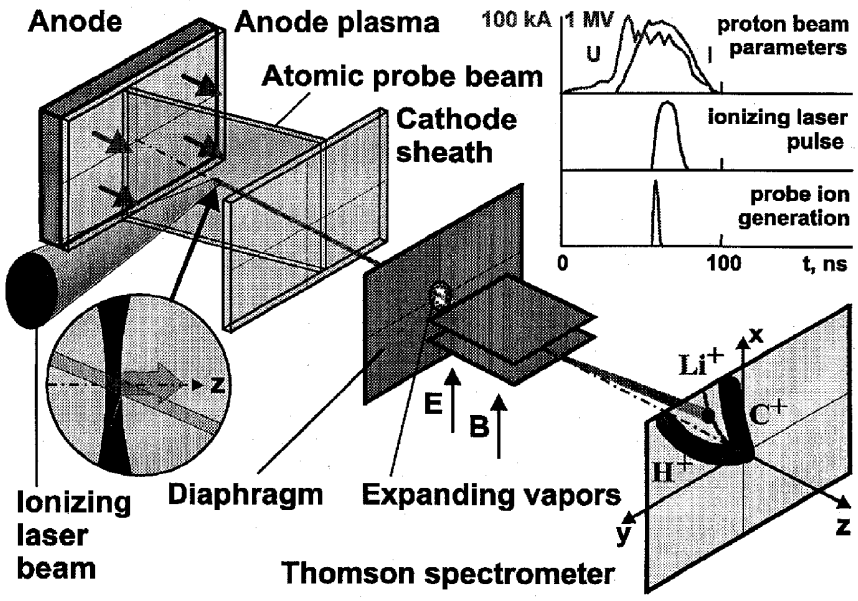

Figure 3: Schematic of local generation of probe ions in the diode and Thomson spectrometer detector system.

voltage and current, ionizing laser pulse, and pulse of probe ions for such case are presented in the right top corner of Fig. 3. Total number of probe ions produced is $N_{pi} = 4 \cdot 10^6$.

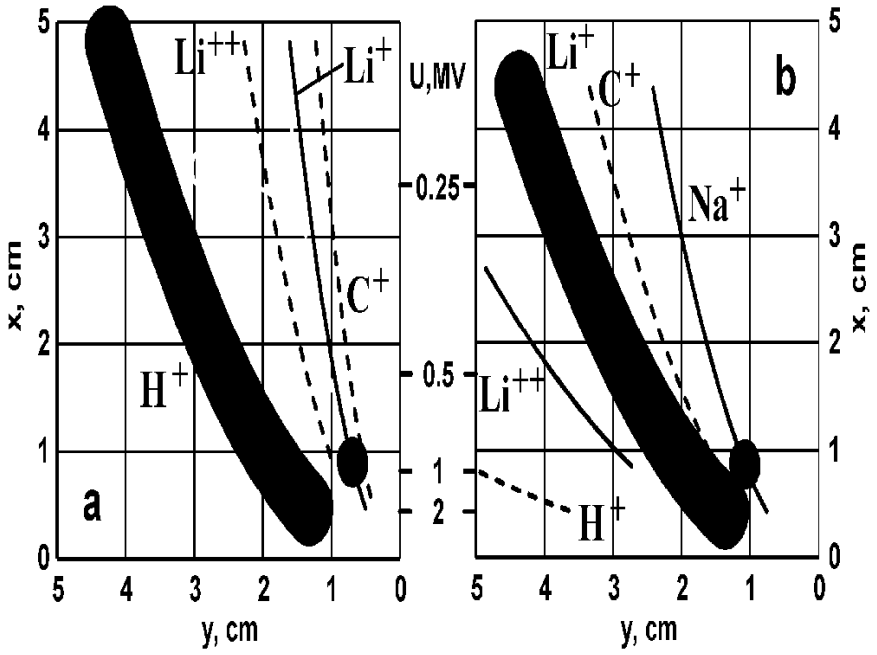

Figure 4: Calculated ion traces on the detector of a Thomson spectrometer: (a) proton diode and lithium probe ions with $a = 5$ cm plate length, $l = 30$ cm from plates to detector, $aE = 7 \cdot 10^4$ V, $aB = 1 \cdot 10^4$ G·cm; (b) lithium diode and sodium probe ions with $a = 10$ cm, $l = 30$ cm, $aE = 7 \cdot 10^4$ V, $aB = 3 \cdot 10^4$ G·cm. We assumed input hole diameter of 3mm, and a divergence of the bulk beam of 15 mrad.

For this system, a Thomson spectrometer, as shown in Fig. 3, is an adequate detector. One of the disadvantages of the conventional Thomson spectrometer, which complicates measurement of the beam divergence, is the necessity to collimate an intense ion beam by means of a pinhole. Evaporated material expanding into the hole can absorb and scatter the ions and disturbs results of measurement of energy and divergence. A great advantage of LPID is the capability to study probe beam divergence without any material colli-

mating holes and slits, because the probe ions can be produced in the diode in a small volume. For this reason one may use a spectrometer with a large input aperture (Fig. 3) adjusted with the axis of probe ion beam. Other beam ion species are recorded as thick parabolas, whereas the probe ions, locally produced for a time τ_i, produce a small spot. Position of the spot on the corresponding parabola gives the potential at the point of ionization.

The spot size is governed by the transverse velocity obtained during acceleration and drift from point of ionization in the diode to the spectrometer. For proton beam current $I_b = 25$ kA and anode cross-section $S_a = 300$ cm^2 proton density in the diode is about $5 \cdot 10^{11}$ cm^{-3}. Density of probe lithium ions for $N_{pi} = 4 \cdot 10^6$, $\tau_i = 1$ ns and $S_{pi} = 2 \cdot 10^{-4}$ cm^2 is $0.8 \cdot 10^{11}$ cm^{-3}, and one can neglect influence of its space charge. Thus, because the velocity of probe atoms is very low, the size of the spot on the detector plane corresponds to probe beam divergence. Dependence of the spot size as a function of point of ionization maps the transverse disturbance of the beam across the gap.

Neglecting boundary effect, coordinates on the detector plane of an ion with a kinetic energy $T = ZeU$, ion charge Z and mass A can be found from the expressions

$$x\,[\mathrm{cm}] = \frac{5.0 \cdot 10^{-7}\, Z\,(aE\,[\mathrm{V}])(l - a/2)}{T\,[\mathrm{MeV}]}\,, \tag{14}$$

$$y\,[\mathrm{cm}] = \frac{6.9 \cdot 10^{-6}\,(aB\,[\mathrm{G{\cdot}cm}])(l - a/2)\,Z}{\sqrt{A}\,\sqrt{T\,[\mathrm{MeV}]}}\,, \tag{15}$$

where a is length of the electric and magnetic fields E and B in the spectrometer (see, Fig. 2), l is distance from beginning of the fields to the detector plane.

As a specific example, we describe here a detector system constructed at Novosibirsk State University for this diagnostic. We use a two-part detector. A CR-39 film records the parabolas produced by bulk ions. This film has a parabolic opening along the probe-ion trace. As a sensitive detector for the probe ions we place behind the CR-39 a gated microchannel plate (MCP) with acceleration gap and scintillator at the output. Characteristics of the Thomson spectrometer (see *i.e.* [14]) are matched to the size of the MCP. Assuming diameter of MCP to be 5 cm, we selected parameters of spectrometer for probe lithium ions in proton-beam diode and probe sodium ions in lithium beam diode. These parameters are given in the caption to Fig. 4, where parabolas for the bulk and probe ions are drawn. A width of the bulk ion trace is a sum of the collimator diameter (2 mm) and the beam

divergence. The width of the trace in the figure corresponds to 15 mrad, which in accordance with review [15] is minimum magnitude for existing ion accelerators.

Probe ions produce a localized spot on the detector. In the figure we assume divergence of the probe beam equal to 10 mrad. Position of the spot on the x-axis gives the potential at the starting point of the probe ions. The Li^+ trace must be resolved from C^{++}, which is a universal component in ion diodes. On the spot area of 0.1 cm^2 we have $4.5 \cdot 10^4$ pixels of MCP. To obtain reasonable dynamic range, not more then 10% of the MCP channels must work during a pulse [16]. Because efficiency of ion detection by MCP is 4–60% [17] we need not more then 10^5 ions to record areal distribution of probe ions. This value is much less then $N_{pi} = 5 \cdot 10^6$ calculated above, and probably, these ions can be detected simply with CR-39. However, additional advantage of MCP is possibility to escape over-irradiation of detector with unwanted ions by gating the MCP.

The combined spectroscopic and particle diagnostic described in this paper, which allows simultaneous study of both electric field distribution in the diode and divergence of the bulk beam and probe ion beam with excellent space and time resolution. It is very reliable, because probe ion signal can be obtained only when the atomic probe beam, the exciting laser(s), and the ionizing laser are "switched on". The absence of any of them excludes appearance of useful signal. For this reason the LPID can be classified is a "triply active" diagnostics.

Acknowledgments

This material is based upon work partially supported by grants of U.S. Civilian Research and Development Foundation (Award RP1-239), the Ministry of General and Professional Education of Russian Federation, and the program "Integration of Science and Education" (grant No. 274). One of the authors is indebted to H. Bluhm for helpful discussions.

References

[1] Y. Maron, M.D. Coleman, D. Hammer, H.-S. Peng. Phys. Rev. Lett., **57**, 699 (1986).

[2] J. Bailey, A. Filuk, A.L. Karlson *et.al. Atomic processes in plasmas. Tenth Topical Conference*, San Francisco, 1996. AIP Conf. Proc. **381**, 245 (1996).

[3] B.A. Knyazev, S.V. Lebedev, P.I. Melnikov. *Proc. 17-th Internat. Conf. on Phenomena in Ionized Gases*, Budapest, 1985, V. 2, P. 1008.

[4] B.A. Knyazev, S.V. Lebedev, P.I. Melnikov. Zh. Tekh. Fiz. **61**, 6 (1991) [Sov. Phys. Tech. Phys., **36**, 250 (1991)].

[5] B.A. Knyazev, S.V. Lebedev, P.I. Mel'nikov. Pis'ma Zh. Tekh. Fiz. **17**, 16 (1991) [Sov. Tech. Phys. Letters, **17**, 357 (1991)].

[6] V.V. Chikunov, B.A. Knyazev, P.I. Melnikov. *Proc. 9-th Internat. Conf. on High-Power Particle Beams*, Washington, 1992, V. 2, P. 1043.

[7] B.A. Knyazev, P.I. Melnikov, J.B. Greenly, D.A. Hammer. *Abstracts of 8th Internat. Workshop on Atomic Physics for Ion-Driven Fusion*, Heidelberg, Germany, 1997, P. 67.

[8] B.A. Knyazev, P.I. Melnikov. *9-th Europ. Sect. Conf. on Atomic and Molecular Phenomena in Ionized Gases*, Lisbon, 1988, Europhys. Conf. Abstracts, V. 12H, P. 299 (1988).

[9] B.A. Knyazev, W. An, H. Bluhm, L. Buth. *Abstracts of 12th Internat. Conf. on High-Power Particle Beams*, Haifa, Israel, June 1998, P. 172.

[10] I.A.Dolbnya, G.G. Fel'dman, B.A. Knyazev, V.P. Simonov. Nuclear Instr. and Methods, **A308**, 435 (1991).

[11] H. Griem. *Principles of plasma spectroscopy.* Cambridge University Press, Cambridge, 1997.

[12] D. Kleppner, M. Littman, M. Zimmerman. In *Ridberg states of atoms and molecules.* Ed. by R.F. Stebbings and F.B. Dunning. Cambridge University Press, Cambridge, 1983.

[13] A.G. Leonov, A.N. Starostin, D.I. Chekhov. JETP **111**, 703 (1997).

[14] R.F. Schneider, C.M. Luo, M.J. Rhee. J. Appl. Phys., **57**, 1 (1985).

[15] C.L. Olson, M.E. Cuneo, M.P. Desjarlais et al. *Proc. 11-th Internat. Conf. on High Power Particle Beams*, Prague, 1996, V. 1, P. 104.

[16] B.A. Knyazev. Instruments and Experimental Techniques, **34**, 191 (1991).

[17] J.L. Wiza. Nucl. Insrum. and Methods, **162**, 587 (1979).